Molecular genetics and the evolution of ultraviolet vision in vertebrates

Yongsheng Shi, F. Bernhard Radlwimmer, and Shozo Yokoyama*

Department of Biology, Syracuse University, 130 College Place, Syracuse, NY 13244

Edited by Jeremy Nathans, Johns Hopkins University School of Medicine, Baltimore, MD, and approved August 1, 2001 (received for review May 23, 2001)

Despite the biological importance of UV vision, its molecular bases are not well understood. Here, we present evidence that UV vision in vertebrates is determined by eight specific amino acids in the UV pigments. Amino acid sequence analyses show that contemporary UV pigments inherited their UV sensitivities from the vertebrate ancestor by retaining most of these eight amino acids. In the avian lineage, the ancestral pigment lost UV sensitivity, but some descendants regained it by one amino acid change. Our results also strongly support the hypothesis that UV pigments have an unprotonated Schiff base-linked chromophore.

It is now clear that, counter to the traditional view, many vertebrates use UV vision for such basic behaviors as foraging, social signaling, and mating (1–5). UV vision is achieved by the pigments that absorb light maximally (λ_{max}) at ≈360 nm, but the mechanisms of the spectral tuning in these UV pigments remain mostly as an area of speculation. In general, visual pigments consist of an apoprotein, opsin, and an 11-*cis*-retinal chromophore that is bound to opsin by a Schiff base linkage to the lysine residue in the center of the seventh transmembrane (TM) helix (6). The Schiff base of 11-*cis*-retinal is usually protonated by the glutamate counterion in the third TM helix (7–9). The protonated Schiff base has a λ_{max} at 440 nm in solution (10). Through the interaction with an opsin, however, the Schiff base-linked chromophore in a visual pigment can have a λ_{max} ranging from 360 to 635 nm (11). Interestingly, the unprotonated Schiff base-linked chromophore in solution has a λ_{max} at 365 nm (12). Thus, it has been proposed that UV pigments may have an unprotonated Schiff base-linked chromophore (13–17), but this hypothesis has not been experimentally tested.

Recently, it has been shown that some avian species have acquired UV vision by one amino acid change (17, 18). It is also proposed that five amino acid sites regulate the absorption spectra of UV pigments in nonavian species (19). This evolutionary approach, however, lacks rigor in identifying all amino acids involved in the spectral tuning in the UV pigments. Here, to study the molecular bases of UV vision, we first determine the mechanisms of the spectral tuning in the mouse UV pigment. The general molecular bases of UV vision in vertebrates are then studied by considering the mouse UV pigment and other orthologous pigments, often referred to as short-wavelength-sensitive type 1 (SWS1) pigments (20, 21). Using the mouse UV pigment, we also examine the effects of the glutamate counterion on the spectral sensitivities of visual pigments.

Materials and Methods

Construction of Chimeric Pigments and Site-Directed Mutagenesis. The UV opsin cDNA clone of the mouse (*Mus musculus*) has been subcloned into an expression vector, pMT5 (22). The human blue opsin cDNA clone is a gift from Jeremy Nathans (Johns Hopkins Univ., Baltimore). To subclone the human blue opsin cDNA into pMT5, the cDNA clone was amplified by PCR by using primers: 5′-AGGGTGGAATTCCACCATG-AGAAAAATGTCGGAGG-3′ (forward) and 5′-GGTCCT-GTCGACGGGCCAACTTGGGTAGACG-3′ (reverse).

We have constructed a series of chimeras between the mouse UV opsin and human blue opsin by recombining them at restriction sites *Msc*I (located at codon 56 of the mouse UV opsin gene), *Pvu*II (codon 93), *Sph*I (codon 147), and *Bam*HI (codon 254). Point mutations were generated by using the QuickChange site-directed mutagenesis kit (Stratagene). The mutant cDNA clones were sequenced to rule out spurious mutations, and desired mutants were subcloned into the expression vector pMT5.

Spectral Analyses of Pigments and Sequence Data Analyses. The opsin cDNAs in pMT5 were expressed in COS1 cells by transient transfection. The visual pigments were then regenerated by incubating the opsins with 11-*cis*-retinal (Storm Eye Institute, Medical University of South Carolina, Charleston) in the dark (for more details, see ref. 23). The resulting visual pigments were then purified by immunoaffinity chromatography by using monoclonal antibody 1D4 Sepharose 4B (The Cell Culture Center, Minneapolis, MN) in buffer consisting of 50 mM *N*-(2-hydroxyethyl) piperazine-*N*′-2-ethanesulfunic acid (pH 6.6), 140 mM NaCl, 3 mM $MgCl_2$, 20% (wt/vol) glycerol, and 0.1% dodecyl maltoside. UV-visible absorption spectra of the visual pigments were recorded at 20°C by using a Hitachi (Tokyo) U-3000 dual beam spectrophotometer. Visual pigments were bleached by a 366-nm UV light illuminator and a 60-W room lamp with 440-nm cutoff filter. They were also denatured by sulfuric acid (H_2SO_4) at pH 1.8 in the dark. Recorded spectra were analyzed by using SIGMAPLOT software (Jandel, San Rafael, CA).

Previously, we have studied the phylogenetic relationships of 17 SWS1 pigments from Malawi fish (*Metriachlima zebra*), goldfish (*Carassius auratus*), zebrafish (*Danio rerio*), clawed frog (*Xenopus laevis*), chicken (*Gallus gallus*), pigeon (*Columba livia*), parakeet (*Melopsittacus undulatus*), zebra finch (*Taeniopygia guttata*), canary (*Serinus canaria*), chameleon (*Anolis carolinensis*), human (*Homo sapiens*), macaque (*Macaca fascicularis*), squirrel monkey (*Saimiri boliviensis*), marmoset (*Callithrix jacchus*), bovine (*Bos taurus*), mouse (*Mus musculus*), and rat (*Rattus norvegicus*) (19). The ancestral amino acid sequences were inferred by a likelihood-based Bayesian method (24) by using a modified version of the Jones, Taylor, and Thornton model, the Dayhoff model, and the equal-input model (for more details, see ref. 19).

Results and Discussion

Spectral Tuning of Mouse UV Pigment. Apart from the two fewer N-terminal amino acids in the mouse UV pigment, the amino acids of the mouse UV and human blue opsins differ at 50 sites (Fig. 1 *A* and *B*). The human blue and mouse UV pigments have λ_{max} values of 414 nm (Fig. 2*A*; ref. 25) and 359 nm (Fig. 2*E*; ref. 22), respectively. Using appropriate restriction enzymes (Fig. 1*B*), we constructed chimeric pigments m(93)h, m(147)h,

This paper was submitted directly (Track II) to the PNAS office.

Abbreviations: TM, transmembrane; SWS1, short-wavelength-sensitive type 1.

*To whom reprint requests should be addressed. E-mail: syokoyam@mailbox.syr.edu.

The publication costs of this article were defrayed in part by page charge payment. This article must therefore be hereby marked "*advertisement*" in accordance with 18 U.S.C. §1734 solely to indicate this fact.

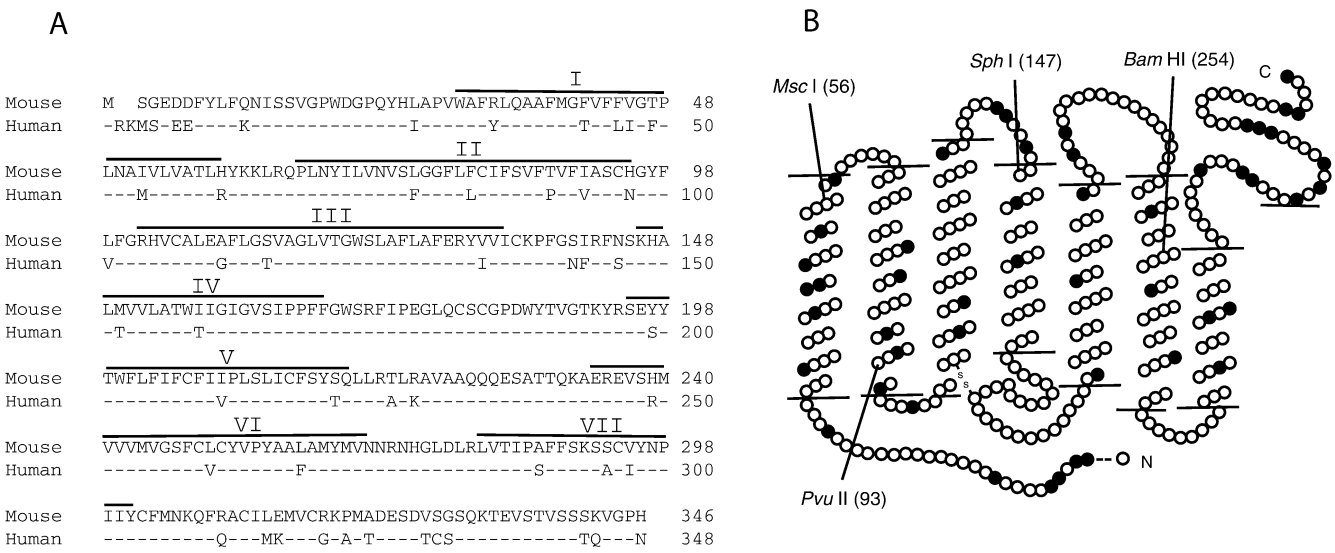

Fig. 1. Sequence comparison between mouse UV pigment and human blue pigment. (*A*) The aligned amino acid sequences of the two pigments. Dashes (—) indicate the identity of the amino acids with those of mouse UV pigment. (*B*) Topographical structure with seven TM helices (adapted from ref. 27), where filled circles indicate differences between the two pigments.

m(254)h, h(93)m, h(147)m, and h(254)m, where amino acids 93–346, 147–346, 254–346, 1–92, 1–146, and 1–253 of the mouse pigment are replaced by the corresponding segments of the human pigment, respectively. The λ_{max} of m(93)h, m(147)h, and m(254)h pigments are 365, 360, and 360 nm, respectively (Fig. 2 *B–D*), whereas those of h(93)m, h(147)m, and h(254)m pigments

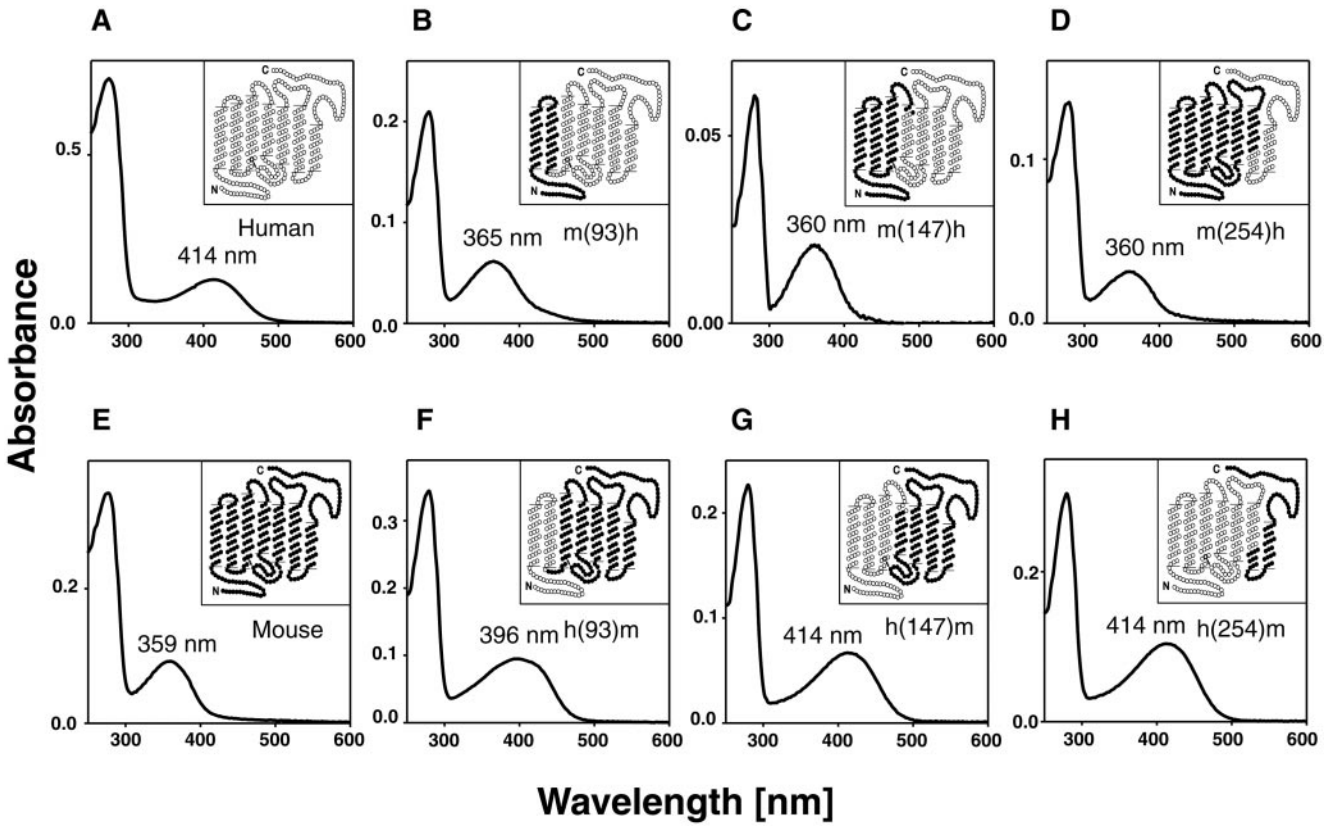

Fig. 2. Absorption spectra of human blue pigment (*A*), mouse UV pigment (*E*), and chimeric pigments (*B–D*, *F–H*). The pigment structures are shown in the *Insets*. The residues from mouse UV pigment are shown as filled circles, and those from human blue pigment as open circles. When all of these pigments are exposed to light and denatured by sulfuric acid (H_2SO_4) in the dark, new peaks at ≈380 and 440 nm are attained, respectively. These control experiments demonstrate that the observed lower peaks are due to opsins covalently linked to 11-*cis*-retinal via a Schiff base bond. The λ_{max} values of the pigments are found near the peaks of the absorption spectra curves. Note that, unlike typical bell-shaped spectra (*A–E*, *G*, and *H*), the absorption spectrum of h(93)m pigment has a second minor peak at ≈410 nm (*F*). This may occur because of the coexistence of visual pigments with unprotonated and protonated Schiff bases (7, 8).

are 396, 414, and 414 nm, respectively (Fig. 2 *F–H*). These results clearly demonstrate that the first 146 amino acids from the N terminus of the mouse UV pigment are responsible for its spectral sensitivity.

When the 146 amino acids of the mouse UV pigment and the corresponding segment of the human blue pigment are compared, we find amino acid differences at 25 sites (Fig. 1 *A* and *B*). Among these, the last 19 sites, starting with TM helix I, are located within or near the TM segments, where most interactions between the 11-*cis*-retinal and the opsin seem to take place (20, 21). Thus, it is strongly suspected that some of these 19 sites are responsible for spectral tuning in the mouse UV pigment. Accordingly, we introduced 19 single human blue pigment-specific amino acid changes into the corresponding positions of the mouse UV pigment. Following the amino acid site numbers of the bovine rhodopsin, these amino acid changes are R38Y, F46T, F49L, V50I, T52F, I57 M, H64R, L81F, F86L, T93P, I96V, H100N, L104V, A114G, S118T, V137I, S145N, I146F, and N149S. Much to our surprise, however, we found that none of these single mutations shifts the λ_{max} value from that of the mouse UV pigment, 359 nm (Fig. 3).

To evaluate the interactions of various amino acids, we then constructed three additional chimeric pigments, m(56)h(93)m, m(93)h(147)m, and m(56)h(147)m, where the amino acid sites 56–92 (including TM helix II), 93–146 (TM helix III), and 56–146 (TM helices II and III) of the mouse pigment are replaced by the corresponding sites of the human pigment, respectively. The λ_{max} of m(56)h(93)m, m(93)h(147)m, and m(56)h(147)m pigments are 381, 363, and 405 nm, respectively (Table 1). Again following the amino acid site numbers of the bovine rhodopsin, these values are fully explained by L81F/F86L/T93P (amino acid changes L81F, F86L, and T93P), A114G/S118T, and L81F/F86L/T93P/A114G/S118T (Table 1, Fig. 3). Similarly, the λ_{max} of h(93)m pigment is explained by F46T/F49L/T52F/L81F/F86L/T93P (Table 1, Fig. 3). It should be noted, however, that many pigments with multiple mutations exhibit somewhat abnormal absorption spectra with an additional minor peak at ≈410 nm (Table 1, Fig. 3; see also Fig. 2*F*). We have attempted to narrow the width of the absorption spectrum by subjecting the mouse UV pigment with F86L/T93P to various pH conditions. However, at pH 4.0, 4.9, 5.6, 6.9, 7.4, 8.2, and 8.3, the mutant pigment shows identical absorption spectra (result not shown).

These mutagenesis results strongly suggest that the amino acids at the eight sites in TM helices I–III are responsible for spectral tuning in mouse UV pigment. In fact, when F46T/F49L/T52F/L81F/F86L/T93P/A114G/S118T are introduced into mouse UV pigment, the mutant pigment achieves a λ_{max} at 412 nm (Fig. 3), whereas the human pigment with the reverse mutations has a λ_{max} of 359 nm (result not shown). Among these eight amino acids changes, L81F is least effective in shifting the λ_{max}. For example, F86L/T93P shift the λ_{max} 19 nm toward blue, but the addition of L81F increases the blue shift by only 3 nm. In addition, neither L81F/F86L nor L81F/T93P cause any λ_{max} shift (Fig. 3). Indeed, the mouse UV pigment with seven mutations F46T/F49L/T52F/F86L/T93P/A114G/S118T achieves a λ_{max} at 411 nm (Figs. 3 and 4*A*), whereas the human blue pigment with the reverse mutations achieves a λ_{max} at 360 nm (Figs. 3 and 4*B*). These λ_{max}s are practically identical to those of the corresponding pigments with the eight mutations. Thus, the difference in the λ_{max} between the mouse and human pigments is explained fully by the amino acid differences at sites 46, 49, 52, 86, 93, 114, and 118. Another site 90 is also known to have contributed significantly to the evolution of avian UV pigments (17, 18). Among these eight sites, 46, 49, 52, 86, 90, 93, and 114 are located near the Schiff base nitrogen and 118 near C-11 of the 11-*cis*-retinal chromophore (26, 27).

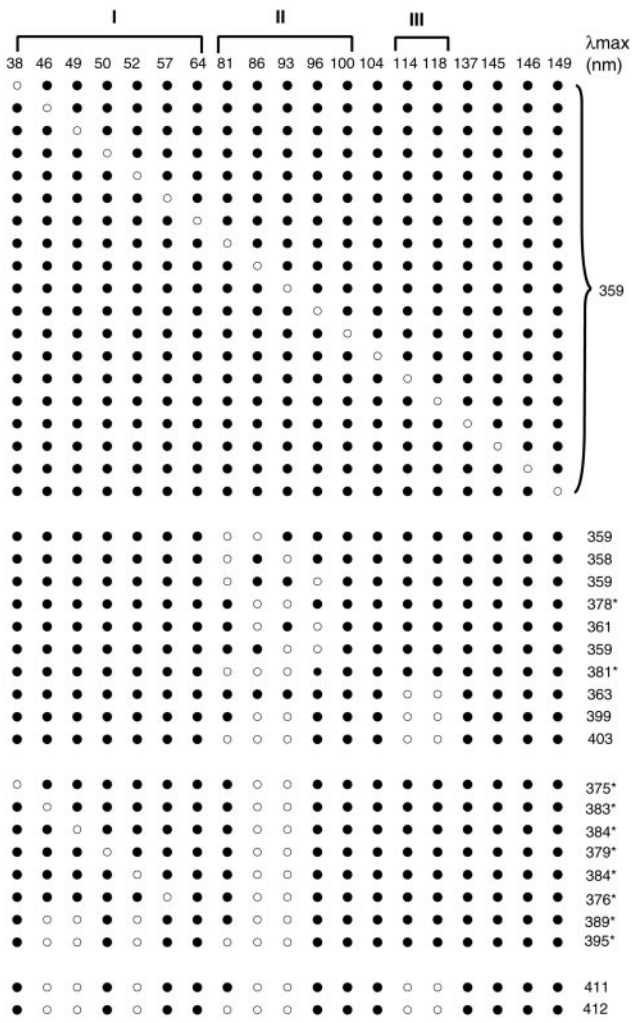

Fig. 3. Schematic representation of the point mutations of the mouse UV pigment. A solid circle indicates an unchanged amino acid, whereas an open circle indicates the change from the amino acid of the mouse pigment to that at the corresponding site of the human pigment. Both photobleaching and acid denaturation experiments show that the λ_{max} values are indeed due to mutant visual pigments. The λ_{max} values of the mutants are shown in the last column. The standard errors associated with these estimates are all within 1 nm. The λ_{max} values marked with a star (*) indicate that their absorption spectra have a second minor second peak at ≈410 nm (see also Fig. 2*F*).

Molecular Evolution of the SWS1 Pigments. To derive the general genetic rule underlying UV vision in vertebrates, it is necessary to study the effects of the eight critical sites on the spectral tuning in other orthologous pigments. For that purpose, we use the

Table 1. Summary of the λ_{max} values of the mutant mouse UV pigments

Visual pigment	TM	λ_{max}, nm
m(56)h(93)m	II	381*
L81F/F86L/T93P	II	381*
m(93)h(147)m	III	363
A114G/S118T	III	363
m(56)h(147)m	II and III	405
L81F/F86L/T93P/A114G/S118T	II and III	403
h(93)m	I and II	396*
F46T/F49L/T52F/L81F/F86L/T93P	I and II	395*

*Absorption spectrum has a second peak at ≈410 nm.

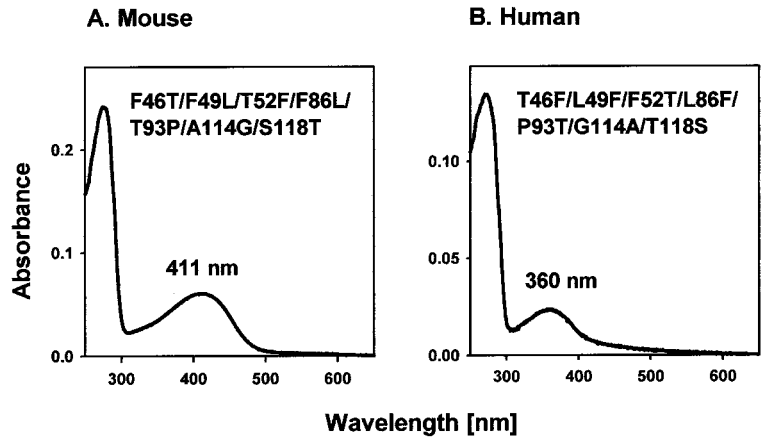

Fig. 4. Absorption spectra of the mouse UV pigment with the seven mutations (*A*) and human blue pigment with the reverse mutations (*B*).

results on the previous phylogenetic analyses of the SWS1 pigments from 17 species (19).

The Jones, Taylor, and Thornton, Dayhoff, and equal-input models of amino acid replacements predict that the amino acids at the eight critical sites in the pigment of the vertebrate ancestor are F46/F49/T52/F86/S90/T93/A114/S118 (Fig. 5). This amino acid composition is identical to those of the chameleon, mouse, and rat UV pigments, but it differs from those of the three fish UV pigments by one common amino acid at site 93. It turns out, however, that the goldfish UV pigment with Q93T does not shift the λ_{max} from 359 nm (19). These observations strongly suggest that the ancestral vertebrate pigment was UV-

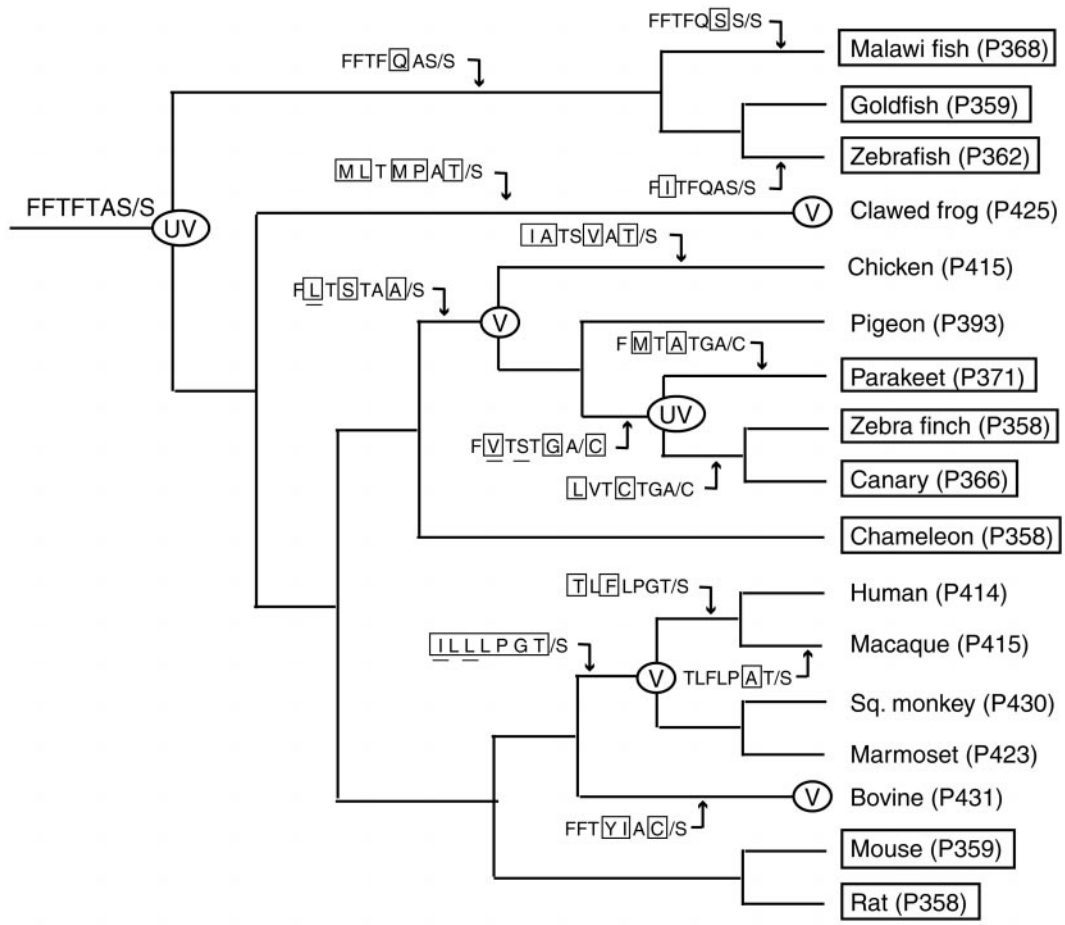

Fig. 5. A composite tree topology of the vertebrate SWS1 pigments (19) and ancestral amino acids inferred by using the Jones, Taylor, and Thornton model of amino acid replacements. The UV pigments are boxed. The five ancestral amino acids with posterior probabilities of 90% or less are underlined. The first seven amino acids next to the branches are those at sites 46, 49, 52, 86, 93, 114, and 118, in that order, whereas the eighth amino acids after a slash (/) are those at site 90, where the site numbers are those of the bovine rhodopsin. The boxes around amino acids indicate amino acid replacements. UV and V indicate UV and violet sensitivities, respectively.

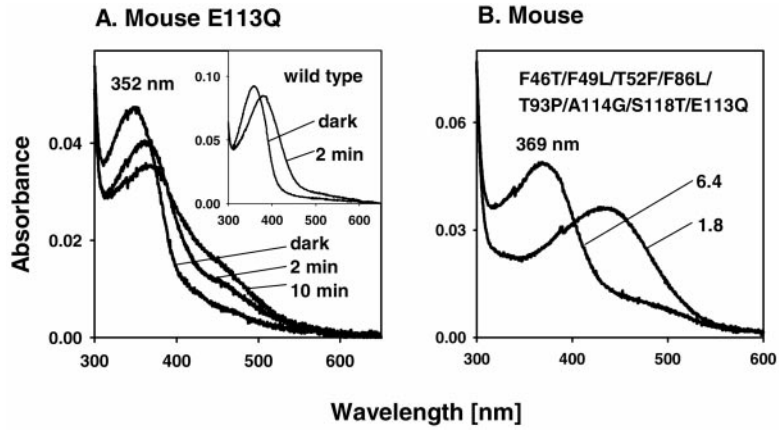

Fig. 6. Absorption spectra of the mouse UV pigment with and without E113Q (*A*) and that with the seven mutations and E113Q (*B*). The spectra in *A* were measured in the dark and after 2 and 10 min of exposure to UV light, whereas those in *B* were measured at pH 6.4 and 1.8.

sensitive, having a λ_{max} of ≈360 nm, and that various violet pigments evolved from the UV pigment.

In the avian lineage, the ancestral pigment has F46/L49/T52/S86/S90/T93/A114/A118, suggesting that F49L/F86S/S118A occurred in the ancestral pigment. The amino acid composition at the eight sites of this ancestral pigment is identical to that of the contemporary pigeon pigment. Thus, the ancestral avian pigment must have had a λ_{max} at ≈395 nm. Interestingly, in parakeet, zebra finch, and canary, the UV pigments evolved from this ancestral pigment by the single amino acid replacement, S90C (17, 18).

In nature, the spectral sensitivity of visual pigments in fish and chameleon can be red-shifted by replacing 11-*cis*-retinal by 11-*cis*-3,4-dehydroretinal (20). However, for UV pigments, the effect of switching the two types of chromophore on the λ_{max} shift is negligible (23). The cone photoreceptors with the SWS1 pigments have transparent oil droplets, and their λ_{max} also are not affected by the oil droplets (28). Thus, UV and violet vision in vertebrates is determined directly by their SWS1 pigments. These observations suggest that contemporary UV vision in nonavian species is inherited from the vertebrate ancestor by maintaining most of the eight critical sites in the UV pigments. On the other hand, the violet (or blue) vision evolved from UV vision by accumulating at least two of the eight critical amino acid changes. We have seen that single amino acid changes in the mouse and goldfish UV pigments do not shift the λ_{max}. On the other hand, a single amino acid change S90C in the avian violet pigment can shift the λ_{max} by ≈35 nm (17). These seemingly contradictory observations can be resolved easily by considering F49L/F86S/S118A/S90C together rather than S90C alone. Indeed, when S90C is introduced into the mouse UV pigment, the mutant pigment has a λ_{max} value of 357 ± 1 nm (result not shown), which is virtually identical to the λ_{max} of the mouse UV pigment.

The Role of the Counterion in the Spectral Tuning of Mouse UV Pigment. To test the role of the glutamate counterion in the spectral tuning of visual pigments, we introduced E113Q into the mouse UV pigment. This mutant pigment achieves a λ_{max} at 352 nm and is still UV-sensitive (Fig. 6*A*, dark). When this pigment is subjected to various pH ranging from 5 to 8.5, its absorption spectrum does not change from 352 nm (result not shown). At pH 4, however, this mutant pigment achieves a λ_{max} at 440 nm and becomes denatured. Thus, the glutamate counterion has little effect on the spectral sensitivity in mouse UV pigment, strongly suggesting that mouse UV pigment has the unprotonated Schiff base-linked chromophore.

When E113Q is introduced into mouse pigment with F46T/F49L/T52F/F81L/T93P/A114G/S118T, a very different picture emerges. This pigment shifts its λ_{max} from 411 to 369 nm (Fig. 6*B*, 6.4). When the pH is lowered from 6.4 to 1.8, the pigment attains a λ_{max} at 440 nm and becomes denatured (Fig. 6*B*, 1.8), strongly suggesting that the observed λ_{max} of 369 nm is generated by the mutant visual pigment. We also attempted to evaluate the effect of various pH on the λ_{max} shift. Unfortunately, the mutant pigment becomes unstable outside neutral pH, where we cannot determine the relationship between pH and the λ_{max} of the pigment unambiguously. Because of the drastic decrease in the λ_{max} caused by E113Q, however, it is most likely that the Schiff base of this mutant pigment is predominantly unprotonated. We also introduced the equivalent mutation (E113Q) into the human blue opsin, but the mutant opsin failed to bind to 11-*cis*-retinal (see also ref. 25). However, because the λ_{max} of the human blue pigment is very close to that of the mouse pigment with F46T/F49L/T52F/F86L/T93P/A114G/S118T, it is highly likely that the human blue pigment also has a protonated Schiff base (11).

If the glutamate counterion is not used for the protonation of the Schiff base, why does the mouse UV pigment have E113? When exposed to UV light for 2 min, the mouse UV pigment with E113Q shifts its λ_{max} from 352 nm to ≈370 nm and reveals another peak at 460 nm (Fig. 6*A*, 2 min). After 10 min of UV exposure, its λ_{max} reaches 380 nm, but the 460-nm peak still remains (Fig. 6*A*, 10 min). Such exceptionally stable metal I-like intermediates have also been reported for the UV pigment in the R7 photoreceptor of *Drosophila* (29), which is known to lack the counterion glutamate residue (30, 31). Compared with these, wild-type mouse UV pigment achieves a single peak at 380 nm even after 2 min of UV exposure (Fig. 6*A Inset*). Thus, although it has very little effect on the λ_{max} shift, the counterion in the mouse UV pigment seems important in photobleaching and possibly subsequent phototransduction.

Removal of water molecules from the Schiff base pocket could result in displacement of positive charge away from the Schiff base nitrogen, leading to deprotonation of the Schiff base (32–35). Thus, being responsible for the spectral tuning of the SWS1 pigments, some of the eight critical amino acid differences may be responsible for the trafficking of waters at the Schiff base pocket. In particular, amino acids at 86, 90, and 93 in the TM helix II, located near the Schiff base, have a major impact on the λ_{max} shift (Fig. 3; ref. 17) and may be important in the movement of water molecules in that region. According to hydrophobicity scales of amino acids that incorporate the conformational and environmental factors (36), the hydropathic indices are 5.5

kcal/mol for the F86/S90/T93 of the ancestral vertebrate UV pigment and contemporary chameleon, mouse, and rat UV pigments. Indeed, these values are highest among all ancestral and contemporary SWS1 pigments, which show the highest level of hydrophobicity. The amino acids at sites 46, 49, 52, 86, 90, 93, and 114, located near the Schiff base, of these four UV pigments also show the highest level of hydrophobicity among all ancestral and contemporary SWS1 pigments.

We have also seen that the evolution of violet pigments from the ancestral vertebrate UV pigment requires at least two amino acid changes at the eight critical sites. These strong synergistic interactions may occur because of the highly limited access of water molecules to the Schiff base pocket (33). Although we cannot offer a structural explanation for this stable structural environment of the unprotonated Schiff base, it is conceivable that the introduction of water molecules to this restricted area requires at least two new hydrophilic amino acids. These amino acids may be used to form a new hydrogen-bonding network of water molecules and the peptide backbone (37). In the fish lineage, the corresponding hydropathic index has been reduced from 5.5 to 0.2 kcal/mol due to T93Q. Without recruiting additional appropriate hydrophilic amino acid(s), however, the fish UV pigments can still have an unprotonated Schiff base. The ancestral avian pigment achieved F49L/F86S in the Schiff base pocket, which is still found in the pigeon pigment (Fig. 5). The changes to these relatively more hydrophilic amino acids might have allowed water molecules to move into the Schiff base pocket, generating the protonated Schiff base. When S90 in the pigeon and chicken violet pigments are replaced by a more hydrophobic C90, the mutant pigments become UV-sensitive, possibly due to the depletion of water molecules from the region (17). All of these observations strongly suggest that most of the eight critical amino acid sites are involved directly or indirectly in the protonation and deprotonation of the Schiff base.

We thank J. Belote, P. Dunham, R. Yokoyama, and anonymous reviewers for their comments on an earlier draft of this paper. This work was supported by the National Institutes of Health.

1. Jacobs, G. H. (1992) *Am. Zool.* **342,** 544–554.
2. Burkhardt, D. (1982) *Naturwissenschaften* **69,** 153–157.
3. Fleishman, L. J., Loew, E. R. & Leal, M. (1993) *Nature (London)* **365,** 397.
4. Viitala, J., Korpimaki, E., Palokangas, P. & Koivula, M. (1995) *Nature (London)* **373,** 425–427.
5. Bennett, A. T. S., Cuthill, I.C.& Partridge, J. C. (1996) *Nature (London)* **380,** 433–435.
6. Mathies, R., Oseroff, A. R. & Stryer, L. (1976) *Proc. Natl. Acad. Sci. USA* **73,** 1–5.
7. Sakmar, T. P., Franke, R. R. & Khorana, H. G. (1989) *Proc. Natl. Acad. Sci. USA* **86,** 8309–8313.
8. Zhukovsky, E. A. & Oprian, D. D. (1989) *Science* **246,** 928–930.
9. Nathans, J. (1990) *Biochemistry* **29,** 9746–9752.
10. Kito, Y., Suzuki, T., Azuma, M. & Sekoguchi, Y. (1968) *Nature (London)* **218,** 955–957.
11. Kochendoerfer, G. G., Lin, S. W., Sakmar, T. M. & Mathies, R. A. (1999) *Trends Biochem. Sci.* **24,** 300–305.
12. Ball, S., Collins, F. D., Dalvi, P. D. & Morton, R. A. (1949) *Biochem. J.* **45,** 304–307.
13. Kakitani, H., Kakitani, T., Rodman, H. & Honig, B. (1985) *Photochem. Photobiol.* **41,** 471–479.
14. Fahmy, K. & Sakmar, T. P. (1993) *Biochemistry* **32,** 9165–9171.
15. Harosi, F. I. (1994) *Vision Res.* **34,** 1359–1367.
16. Vought, B. W., Dukkipatti, A., Max, M., Knox, B. E. & Birge, R. R. (1999) *Biochemistry* **38,** 11287–11297.
17. Yokoyama, S., Radlwimmer, F. B. & Blow, N. (2000) *Proc. Natl. Acad. Sci. USA* **97,** 7366–7371.
18. Wilkie, S. E., Robinson, P. R., Cronin, T. W., Poopalasundaram, S., Bowmaker, J. K. & Hunt, D. M. (2000) *Biochemistry* **39,** 7895–7901.
19. Yokoyama, S. & Shi, Y. (2000) *FEBS Lett.* **486,** 167–172.
20. Yokoyama, S. (2000) *Prog. Ret. Eye Res.* **19,** 385–419.
21. Ebrey, T. & Koutalos, Y. (2001) *Prog. Ret. Eye Res.* **20,** 49–94.
22. Yokoyama, S., Radlwimmer, F. B. & Kawamura, S. (1998) *FEBS Lett.* **423,** 155–158.
23. Kawamura, S. & Yokoyama, S. (1998) *Vision Res.* **38,** 37–44.
24. Yang, Z., Kumar, S. & Nei, M. (1995) *Genetics* **141,** 1641–1650.
25. Fasick, J. I., Lee, N. & Oprian, D. D. (1999) *Biochemistry* **38,** 11593–11596.
26. Lin, S. W., Kochendoerfer, G. G., Carroll, K. S., Wang, D., Mathies, R. A. & Sakmar, T. P. (1998) *J. Biol. Chem.* **273,** 24583–24591.
27. Palczewski, K., Kumasaka, T., Hori, T., Behnke, C. A., Motoshima, H., Fox, B. A., Le Trong, I., Teller, D. C., Okada, T., Stenkamp, R. E., *et al.* (2000) *Science* **289,** 739–745.
28. Bowmaker, J. K. (1977) *Vision Res.* **17,** 1129–1138.
29. Stark, W. S., Zuker, C. S. & Rubin, G. M. (1987) *Naturwissenschaften* **63,** 513–518.
30. Montell, C., Jones, K., Zuker, C. S. & Rubin, G. M. (1987) *J. Neurosci.* **7,** 1558–1566.
31. Zuker, C. S., Montell, C., Jones, K., Laverty, T. & Rubin, G. M. (1987) *J. Neurosci.* **7,** 1550–1557.
32. Deng, H., Huang, L., Callender, R. & Ebrey, T. (1994) *Biophys. J.* **66,** 1129–1136.
33. Harosi, F. I. & Sandorfy, C. (1995) *Photochem. Photobiol.* **61,** 510–517.
34. Nagata, T., Terakita, A., Kandori, H., Kojima, D., Shichida, Y. & Maeda, A. (1997) *Biochemistry* **36,** 6164–6170.
35. Rafferty, C. N. & Shichi, H. (1981) *Vision Res.* **33,** 229–234.
36. Engelman, D. M., Steitz, T. A. & Goldman, A. (1986) *Annu. Rev. Biophys. Biophys. Chem.* **15,** 321–353.
37. Nagata, T., Terakita, A., Kandori, H., Schichida, Y. & Maeda, A. (1998) *Biochemistry* **37,** 17216–17222.